The Journal of Neuroscience, June 1, 2002, 22(11):4406–4411

Multiple Mechanisms for the Potentiation of AMPA Receptor-Mediated Transmission by α-Ca^{2+}/Calmodulin-Dependent Protein Kinase II

Jean Christophe Poncer,[1,2] José A. Esteban,[1] and Roberto Malinow[1]

[1]Cold Spring Harbor Laboratory, Cold Spring Harbor, New York 11724, and [2]Institut National de la Santé et de la Recherche Médicale, Cortex and Epilepsie, 75006 Paris, France

Some forms of activity-dependent synaptic potentiation require the activation of postsynaptic Ca^{2+}/calmodulin-dependent protein kinase II (CaMKII). Activation of CaMKII has been shown to phosphorylate the glutamate receptor 1 subunit of the AMPA receptor (AMPAR), thereby affecting some of the properties of the receptor. Here, a recombinant, constitutively active form of αCaMKII tagged with the fluorescent marker green fluorescent protein (GFP) [$\alpha CaMKII_{1-290}$–enhanced GFP (EGFP)] was expressed in CA1 pyramidal neurons from hippocampal slices. The changes in glutamatergic transmission onto these cells were analyzed. AMPA but not NMDA receptor-mediated EPSCs were specifically potentiated in infected compared with nearby noninfected neurons. This potentiation was associated with a reduction in the proportion of synapses devoid of AMPARs. In addition, expression of $\alpha CaMKII_{1-290}$–EGFP increased the quantal size of AMPAR-mediated responses. This effect reflected, at least in part, an increased unitary conductance of the channels underlying the EPSCs. These results reveal that several key features of long-term potentiation of hippocampal glutamatergic synapses are reproduced by the sole activity of αCaMKII.

Key words: synaptic plasticity; CaMKII; viral transfection; silent synapses; AMPA receptors; LTP

Activity-dependent potentiation of synaptic transmission [long-term potentiation (LTP)] in the CA1 field of the hippocampus is apparently expressed through multiple parallel mechanisms converging to enhance AMPA receptor (AMPAR)-mediated synaptic transmission specifically (Kauer et al., 1988; Muller and Lynch, 1988). LTP at excitatory synapses onto these cells is expressed as an increase in the quantal size and quantal content (Malinow and Tsien, 1990; Kullmann and Nicoll, 1992; Liao et al., 1992; Malgaroli and Tsien, 1992, Oliet et al., 1996; Stricker et al., 1996). The increased quantal size may be partly explained by an increased unitary conductance (Benke et al., 1998) and/or an increased number of synaptic AMPAR channels (Hayashi et al., 2000). The increased quantal content may be explained by delivery of AMPA receptors to "silent" synapses that lack functional AMPAR (Kullmann, 1994; Isaac et al., 1995; Liao et al., 1995; Rumpel et al., 1998).

LTP expression relies on a cascade of postsynaptic events, including Ca^{2+} influx through NMDA receptors (NMDARs) and subsequent activation of Ca^{2+}/calmodulin-dependent protein kinase II (CaMKII) (Lisman et al., 1997; Soderling and Derkach, 2000). This oligomeric protein kinase represents a major component of the postsynaptic density (Braun and Schulman, 1995). Autophosphorylation of CaMKII with Ca^{2+}-calmodulin activation leads to a persistent activation of the kinase activity (Miller et al., 1988) and calmodulin trapping (Meyer et al., 1992), thereby prolonging the function of the enzyme beyond the transient rise in intracellular Ca^{2+} concentration. Several arguments support the involvement of CaMKII in LTP generation at glutamatergic synapses. Activated, auto-phosphorylated CaMKII accumulates in dendrites of pyramidal neurons after LTP induction (Fukunaga et al., 1995; Ouyang et al., 1999). Overexpression or direct injection of constitutively active CaMKII in CA1 hippocampal neurons potentiates AMPAR-mediated synaptic transmission and occludes further induction of LTP (Pettit et al., 1994; Lledo et al., 1995; Shirke and Malinow, 1997), whereas genetic suppression of αCaMKII compromises hippocampal LTP (Silva et al., 1992; Hinds et al., 1998). In addition, LTP in CA1 hippocampal neurons is associated with phosphorylation of the AMPAR glutamate receptor 1 (GluR1) subunit (Barria et al., 1997a; Lee et al., 2000). Two (not mutually exclusive) mechanisms have been proposed to explain how CaMKII enhances AMPAR-mediated transmission. In heterologous systems, phosphorylation of GluR1 by CaMKII (Barria et al., 1997b; Mammen et al., 1997) leads to an increased conductance of homomeric GluR1 channels (Derkach et al., 1999). Another mechanism was suggested by experiments indicating that active αCaMKII, as well as LTP, leads to the synaptic translocation of a recombinant GluR1 in CA1 pyramidal neurons (Hayashi et al., 2000).

Despite this wide array of data, it remains unclear whether all modifications of AMPAR-mediated transmission associated with LTP can be attributed solely to increased CaMKII activity. To address this question, we examined several properties of excitatory synaptic transmission onto CA1 pyramidal neurons expressing an activated αCaMKII. We show that expression of this active

Received Jan. 2, 2002; revised March 15, 2002; accepted March 20, 2002.

This work was supported by the Human Frontier Science Program Organization (J.C.P.) and by the Mathers Foundation and the National Institutes of Health (R.M.). We thank Nancy Dawkins-Pisani for technical assistance, Norbert Ankri for providing event detection and analysis software, and Yasunori Hayashi and Richard Miles for critical reading of this manuscript.

Correspondence should be addressed to Roberto Malinow, Cold Spring Harbor Laboratory, 1 Bungtown Road, Cold Spring Harbor, NY 11724, E-mail: malinow@cshl.org, or to Jean Christophe Poncer, Institute National de la Santé et de la Recherche Médicale, Cortex and Epilepsie, 75006 Paris, France, E-mail: jcponcer@biomedicale.univ-paris5.fr.

J. A. Esteban's present address: Department of Pharmacology, University of Michigan Medical School, Ann Arbor, MI 48109.

enzyme specifically potentiates AMPAR- but not NMDAR-mediated transmission onto infected neurons. We compared the proportion of silent synapses onto cells expressing activated αCaMKII and control cells. Although ~50% of glutamatergic synapses onto control cells are functionally silent, this proportion decreases to approximately zero in cells expressing active αCaMKII. This effect is accompanied by an increased quantal size of AMPAR-mediated responses partly attributable to an increased unitary conductance of channels underlying these responses.

MATERIALS AND METHODS

The fusion between $\alpha CaMKII_{1-290}$ and enhanced green fluorescent protein (EGFP) was made by PCR amplification of the coding sequence of αCaMKII from amino acids 1–290 and in-frame insertion into the pEGFP-N1 vector (Clontech, Palo Alto, CA). This construct was expressed in rat hippocampal slices using Sindbis virus (Malinow et al., 1999).

Hippocampal slices were prepared from 10- to 14-d-old rats of either sex. Rats were deeply anesthetized by intraperitoneal injection of ketamine/xylazine and decapitated. Brains were removed and submerged in ice-cold modified artificial CSF (ACSF) containing (in mM): 250 sucrose, 26 $NaHCO_3$, 10 glucose, 4 KCl, 1 $CaCl_2$, and 5 $MgCl_2$, bubbled with 95% O_2 and 5% CO_2. Horizontal slices (350 μm thick) were prepared with a Vibratome and rinsed in culture medium (MEM plus HBSS) containing penicillin and streptomycin. Slices were then placed on a Millicell insert (Millipore, Bedford, MA) bathed with culture medium in a six well cluster. Viral infection was performed under a dissecting scope using a borosilicate glass microelectrode filled with viral solution (titer of $\sim 10^9$ infective particles per milliliter, as determined by infectivity on baby hamster kidney cells) and mounted on a motorized manipulator. Ten to 50 nl of the solution was typically injected into each slice using a General Valve (Fairfield, NJ) PicoSpritzer. Alternatively, a sparse infection of cells easily accessible with a patch pipette could be obtained using a narrow strip of Millipore (Bedford, MA) polytetrafluoroethylene membrane (0.5 × 10 mm) soaked with the viral solution and positioned right above the CA1 pyramidal cell layer. Slices were then placed in a CO_2 incubator and maintained at 35°C overnight.

Expression of $\alpha CaMKII_{1-290}$–EGFP was tested at different times after infection. Infected slices were solubilized in homogenization buffer (25 μl per slice) composed of 10 mM HEPES-NaOH, pH 7.4, 0.5 M NaCl, 10 mM sodium pyrophosphate, 10 mM NaF, 10 mM EDTA, 4 mM EGTA, 0.1 mM PMSF, 2 μg/ml chymostatin, 2 μg/ml leupeptin, 2 μg/ml antipain, 2 μg/ml pepstatin, and 1% Triton X-100. The solution was cleared by centrifugation at 10,000 × *g* for 5 min at 4°C. Supernatants were analyzed by Western blot using anti-αCaMKII antibodies (Roche, Hertfordshire, UK).

For CaMKII assay, slices were homogenized in 50 mM HEPES-NaOH, pH 7.4, 50 mM NaCl, 10 mM sodium pyrophosphate, 10 mM NaF, 1 mM EGTA, 0.5 mM DTT, 0.1 mM PMSF, 2 μg/ml chymostatin, 2 μg/ml leupeptin, 2 μg/ml antipain, 2 μg/ml pepstatin, 10% glycerol, and 1% NP-40 (total volume of 25 μl per slice). The total CaMKII activity in the extracts was assayed with 2 μg of protein extracts. Reaction buffer (25 μl) contained 10 mM HEPES-NaOH, pH 7.4, 10 mM sodium pyrophosphate, 10 mM NaF, 0.5 mM DTT, 5 mM $MgCl_2$, 50 μM ATP, 2 μCi [γ-^{32}P]ATP, 20 μM autocamtide-2 (Calbiochem, La Jolla, CA), 2 mM $CaCl_2$, and 1 μM calmodulin (Calbiochem). To assay Ca^{2+}-independent CaMKII activity, calcium/calmodulin was omitted and 10 mM EGTA was added. Reactions were performed at 30°C for 5 min. These reaction conditions were shown to be linear with protein concentration and incubation time. Reactions were stopped by spotting the mixture on P81 phosphocellulose paper and adding 1% phosphoric acid. Incorporated radioactivity was measured with a scintillation counter.

For recording, slices were transferred to a submerged chamber maintained at 29–31°C and superfused with ACSF containing (in mM): 118 NaCl, 26 $NaHCO_3$, 10 glucose, 1 NaH_2PO_4, 2.5 KCl, 3 $CaCl_2$, and 2 $MgCl_2$, bubbled with 95% O_2 and 5% CO_2. Whole-cell recordings from CA1 pyramidal cells were obtained using borosilicate electrodes (2–5 MΩ) containing (in mM): 115 Cs-methylsulfonate, 10 CsCl, 20 HEPES, 10 EGTA, and 4 Mg-ATP, pH 7.2, 292 mOsm. EGFP fluorescence was monitored using endow-GFP filters (Chroma Technology Corp., Brattleboro, VT). Neighboring infected (fluorescent) and noninfected (nonfluorescent) cells could thus be recorded sequentially. EPSCs were evoked in the presence of bicuculline methochloride (20 μM) after transection between CA3 and CA1 areas. Schaffer collateral–commissural fibers were stimulated extracellularly through a patch pipette located in the stratum radiatum, ~50–100 μm distant from the recorded cell. The same stimulus (ranging 3–10 V in amplitude and 50–100 μsec in duration) was delivered to control and infected cells recorded in sequence. Cells were held at −60 or +40 mV and stimuli were delivered at 0.3 Hz. Signals were filtered at 1 kHz and sampled at 5 kHz using programs written in Axobasic. Data were analyzed using macros written under Visual Basic for Microsoft Excel (Microsoft, Seattle, WA). The amplitude of EPSCs recorded at −60 mV was measured using 3–5 msec windows placed at the peak of the response and immediately before the stimulation artifact. For EPSCs recorded at +40 mV, larger windows were used (15–20 msec ~60 msec after the peak). For display, stimulation artifacts were digitally subtracted.

For the estimation of failure rates, 150–300 EPSCs were collected at +40 and then −60 mV. Density estimates of amplitude distributions were computed using a Gaussian kernel of approximately one-half the variance of baseline noise (Malinow, 1991). Failure rates were estimated as twice the integral of the inferior half of the first peak (centered on 0 pA and corresponding to synaptic failures).

For nonstationary variance analysis of evoked EPSCs (Traynelis et al., 1993; Benke et al., 1998; Linden, 2001), 30–50 EPSCs of 150–200 were selected according to the following criteria: similar amplitude close to the mean, smooth rising phase, complete decay to baseline current devoid of spontaneous EPSCs, and constant latency. Selected events were aligned to their half rise time, peak scaled, and averaged. The variance of the currents was derived from the first ~50 msec after the peak of EPSCs and plotted against the mean current. This plot was fit to the polynomial equation: $\sigma^2 = \gamma V_m M - M^2/n + c$, where σ^2 is the current variance, M is the mean current, V_m is the holding potential (equals the driving force for AMPAR EPSCs, assuming a reversal potential of 0 mV), γ is the unitary conductance of AMPAR channels, n is the average number of channels contributing to the mean current, and c is a constant.

Miniature EPSCs (mEPSCs) were detected and analyzed using Detectivent software written under LabView (kindly provided by N. Ankri and H. Korn, Institut Pasteur, Paris, France). Values are expressed as mean ± SEM. Statistical significance was estimated from Mann–Whitney rank sum tests unless otherwise stated. Drugs were purchased from the following sources: DL-APV and 2,3-dihydroxy-6-nitro-7-sulfonyl-benzo[*f*] quinoxal (Tocris Cookson, Bristol, UK) and bicuculline methochloride and 2-chloro-adenosine (Sigma, St. Louis, MO).

RESULTS

Hippocampal slices were infected at high density with Sindbis virus expressing $\alpha CaMKII_{1-290}$–EGFP within the CA1 area (Fig. 1*A*). The expression of the transgene was checked visually by the fluorescence of EGFP as well as by Western blot at different times after infection. It was typically initially detected between 5 and 12 hr after infection (Fig. 1*B*). Ca-independent kinase activity of protein extracts prepared from the infected area increased by approximately threefold within the same time range (3.1 ± 0.7 of controls; $n = 2$) and remained elevated for at least 24 hr.

To investigate the physiological phenotype associated with $\alpha CaMKII_{1-290}$ expression, hippocampal slices were infected at a lower density. As illustrated in Figure 2*A*, infected cells could then be easily identified by their fluorescence, allowing neighboring infected and noninfected cells to be subsequently recorded. We compared the synaptic response mediated by either AMPAR or NMDAR in neighboring infected and noninfected cells with stimulation of the same Schaffer collateral–commissural afferents. AMPAR-mediated responses were recorded while holding the postsynaptic cell at −60 mV, whereas synaptic currents recorded at +40 mV were largely NMDAR-mediated (Poncer and Malinow, 2001). When cells were infected with Sindbis virus expressing EGFP only, no difference in the amplitude of either AMPAR or NMDAR EPSCs was detected in infected cells compared with noninfected cells (0.92 ± 0.25 of controls at −60 mV, $p = 0.72$, $n = 9$; 1.11 ± 0.35 of controls at +40 mV, $p = 0.84$, $n = 5$) (Fig. 2). In contrast, cells infected with Sindbis virus

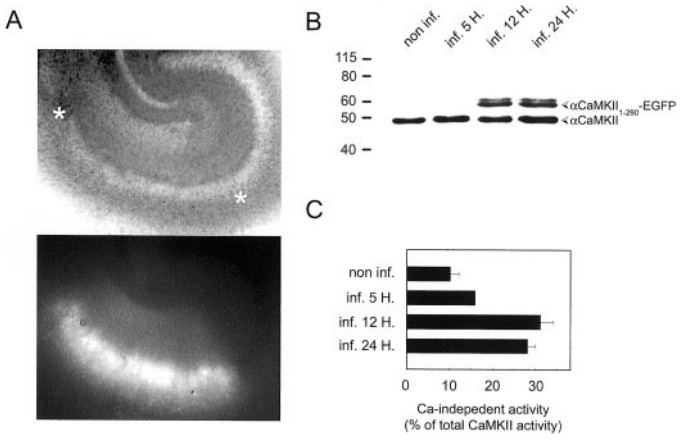

Figure 1. Expression of recombinant αCaMKII in hippocampal slices. *A*, *Top*, Hippocampal slice (see Materials and Methods) after overnight infection with Sindbis virus expressing $\alpha CaMKII_{1-290}$–EGFP. Several injections of the virus were made in the CA1 region (between *asterisks*) resulting in massive expression of the transgene, as detected by fluorescence microscopy (*bottom*). *B*, Western blot of protein extracts from slices at various times after infection. In addition to endogenous αCaMKII (*lower band*), the recombinant fusion protein of higher molecular weight was detectable with αCaMKII antibody between 5 and 12 hr after infection. *C*, In agreement with these results, a kinase assay on cell extracts prepared at various times after infection revealed a significant increase in Ca^{2+}-independent kinase activity between 5 and 12 hr after infection (3.1 ± 0.7 of controls).

expressing the fusion protein $\alpha CaMKII_{1-290}$–EGFP showed a marked increase in AMPAR EPSC amplitude (3.73 ± 0.9 of controls; $p < 0.001$; $n = 13$) with no significant change in the amplitude of NMDAR EPSCs (0.83 ± 0.27 of controls; $p = 0.54$; $n = 12$). These results show that constitutive αCaMKII activity specifically potentiates AMPAR- but not NMDAR-mediated synaptic transmission. We subsequently sought to identify the mechanisms responsible for this specific potentiation of AMPAR-mediated responses.

We first tested whether elevated kinase activity in neurons expressing $\alpha CaMKII_{1-290}$–EGFP could induce delivery of endogenous AMPAR to previously silent synapses (Isaac et al., 1995; Liao et al., 1995). We compared the rate of synaptic transmission failures at −60 and +40 mV in neighboring infected and noninfected neurons. To isolate synaptic transmission failures from stimulation failures, stimulus intensity was set sufficiently high to induce AMPAR responses of at least 20–50 pA with no failures. The adenosine A1-receptor agonist 2-chloro-adenosine (3 μM), which produces an identical presynaptic depressant effect at silent and nonsilent synapses (Poncer and Malinow, 2001), was then added to the perfusion to reduce release probability and therefore favor transmission failures. As described previously (Isaac et al., 1995; Liao et al., 1995), stimulation of Schaffer collateral–commissural synapses onto uninfected CA1 pyramidal neurons resulted in a failure rate at −60 mV that was ~1.5- to twofold higher than at +40 mV (Fig. 3) ($F_{-60}/F_{+40} = 1.72 \pm 0.13$; $n = 8$). However, this ratio was significantly reduced in neurons expressing $\alpha CaMKII_{1-290}$–EGFP (1.18 ± 0.06; $n = 10$; $p < 0.005$). These results suggest that expression of constitutively active αCaMKII in CA1 hippocampal neurons increases AMPAR-mediated transmission at least in part by reducing the proportion of synapses devoid of functional AMPAR. However, this reduction may not be sufficient to account for the approximately fourfold increase in AMPAR EPSC amplitude (Fig. 2), suggesting that other modifications of AMPAR-mediated transmission may be induced by αCaMKII activity.

Changes in quantal size associated with LTP at CA3–CA1 synapses have been reported previously (Liao et al., 1992; Oliet et al., 1996). We therefore compared the quantal size in control neurons and neurons expressing $\alpha CaMKII_{1-290}$–EGFP. To compare quantal events of similar origin and postsynaptic location in infected and uninfected cells, synaptic responses evoked by the same afferent stimulation were recorded in neighboring fluorescent and nonfluorescent cells after substitution of Ca^{2+} for Sr^{2+} in the ACSF. Such substitution results in a desynchronization of transmitter release among activated release sites, thereby leading to the occurrence of quantal events within a few hundred milliseconds of afferent stimulation (Goda and Stevens, 1994; Oliet et al., 1996; Behrends and ten Bruggencate, 1998). These events

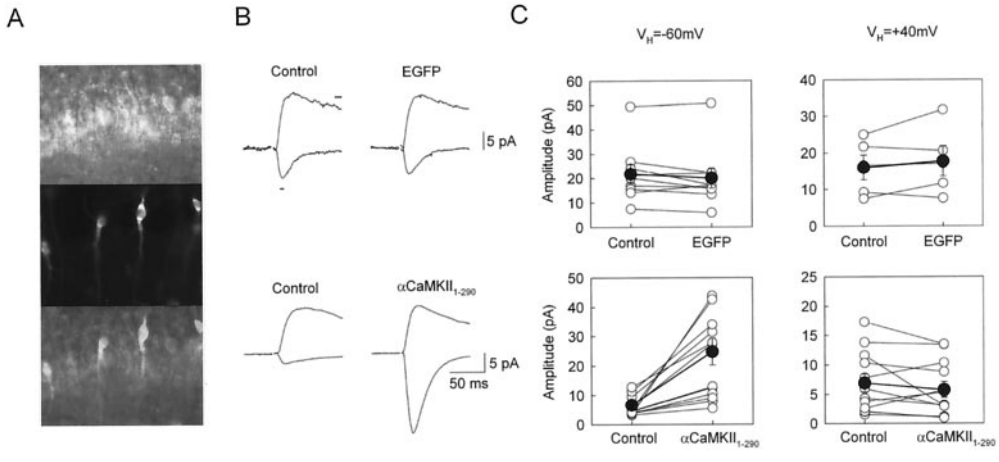

Figure 2. Elevated CaMKII activity selectively potentiates AMPAR- but not NMDAR-mediated synaptic transmission. *A*, Low-density infection of a hippocampal slice. *Top*, Differential interference contrast micrograph of the infected CA1 region. *Middle*, Fluorescence micrograph of the same region showing EGFP fluorescence of infected neurons. Note that only a few CA1 pyramidal neurons were infected. *Bottom*, Superimposition of the two micrographs. *B*, AMPA and NMDAR EPSCs in neighboring infected and noninfected cells. *Top*, CA1 pyramidal cells were infected with Sindbis virus expressing EGFP only. AMPAR-mediated (inward) EPSCs were recorded at −60 mV and were not significantly different in two neighboring infected and noninfected cells. Similarly, EPSCs recorded at +40 mV, primarily carried by NMDAR, were equally unaffected by EGFP expression. *Bottom*, In contrast, when Sindbis virus expressing the fusion protein $\alpha CaMKII_{1-290}$–EGFP was used to infect CA1 neurons, AMPAR EPSCs were greatly increased in amplitude, whereas EPSCs recorded at +40 mV remained unchanged. Each *trace* represents the average of 100 consecutive EPSCs. *Filled bars* show the sections of the *trace* used for amplitude measurements. *C*, Summary plots representing evoked EPSC amplitude in neighboring control and infected cells. *Open circles*, Individual experiments; *filled circles*, averages. The amplitude of both AMPA and NMDAR EPSCs was unchanged in cells expressing EGFP only ($p = 0.72$, $n = 9$ and $p = 0.84$, $n = 5$, respectively). In contrast, expression of $\alpha CaMKII_{1-290}$–EGFP increased the amplitude of AMPAR EPSCs to 3.7 ± 0.9 of controls ($p < 0.001$; $n = 13$) with no effect on NMDAR EPSCs ($p = 0.54$; $n = 12$).

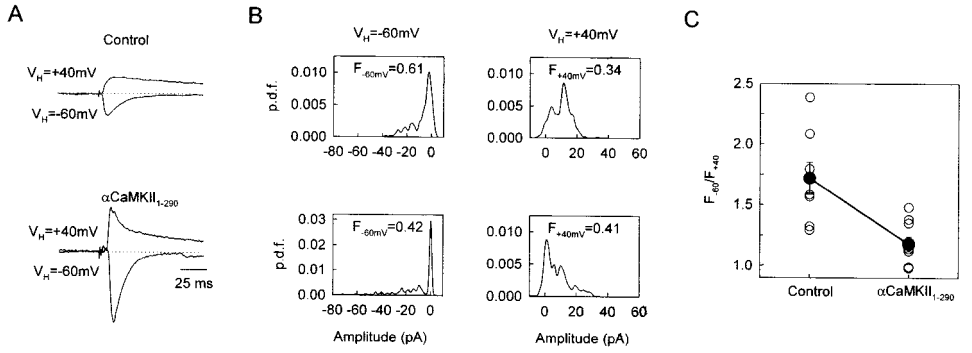

Figure 3. Reduction of the proportion of silent synapses onto pyramidal neurons expressing αCaMKII$_{1-290}$–EGFP. Synaptic failures were counted with stimulation delivered in the stratum radiatum, while holding the cell at either −60 or +40 mV. *A*, One infected cell (*bottom*) and one noninfected cell (*top*) were recorded sequentially. *Traces* were scaled on the amplitude of the EPSC recorded at +40 mV, measured as shown in Figure 2*B*. Each *trace* represents the average of 200 consecutive synaptic responses. *Dotted lines* indicate the baseline current. *B*, Amplitude density estimates of 200 EPSCs from the experiment illustrated in *A*. Failure rates were estimated from the integral of the peak centered on 0 pA. In the control cell, the failure rate recorded at +40 mV was ~45% of that recorded at −60 mV (*top*), whereas no difference was apparent in a neighboring cell expressing αCaMKII$_{1-290}$–EGFP (*bottom*). *p.d.f.*, Probability density function. *C*, Summary plots showing that the ratio of F_{-60} to F_{+40}, describing the proportion of silent synapses, was significantly reduced in cells expressing αCaMKII$_{1-290}$–EGFP ($p < 0.005$; $n = 10$). *Open circles* represent data from individual experiments; *filled circles* show means and SEs.

were preceded by a large, multiquantal event, immediately after afferent stimulation (Fig. 4*A*). Therefore only events occurring within 135–500 msec of synaptic stimulation were measured for this analysis. The mean quantal size of AMPAR EPSCs recorded in these conditions ranged from 4.3–7.5 pA in uninfected cells (mean, 5.9 ± 0.3 pA; $n = 14$). When two neighboring uninfected cells were recorded in sequence, the mean quantal size of EPSCs recorded in both cells was remarkably identical ($p = 0.84$; $n = 4$) (Fig. 4*D*). In contrast, the quantal size of EPSCs recorded from neighboring infected cells reached 9.2–15.8 pA (11.6 ± 0.7 pA; $p < 10^{-5}$; $n = 14$) (Fig. 2*B,C*) with no change in decay kinetics (τ_{decay} = 10.3 ± 0.7 vs 11.3 ± 0.5 for control cells; $p = 0.41$). This effect on quantal size was unlikely to reflect collisions of quantal events because their mean frequency remained low (4.0 ± 1.0 vs 3.2 ± 1.0 Hz in control cells).

Increased quantal size in neurons expressing αCaMKII$_{1-290}$–EGFP could reflect an increased number of receptors per synapse, an increased unitary conductance of AMPAR channels, or both. Constitutive αCaMKII activity has been shown to increase homomeric GluR1 channel conductance in a heterologous expression system (Derkach et al., 1999). We therefore compared the conductance of synaptically activated AMPAR in infected and uninfected neurons. EPSCs of similar amplitude were evoked in neighboring neurons and were used to perform nonstationary variance analysis (see Materials and Methods). The unitary conductance of channels underlying these EPSCs ranged from 8–15 pS in control cells (mean, 11.0 ± 0.8 pS; $n = 9$), as described previously for locally evoked, dendritic EPSCs onto CA1 pyramidal cells (Benke et al., 1998). In cells expressing αCaMKII$_{1-290}$–EGFP, the conductance of channels underlying evoked EPSCs was significantly increased compared with controls and ranged from 14–25 pS (mean, 16.9 ± 1.3 pS; Student's *t* test; $p < 0.002$) (Fig. 5), suggesting that the biophysical properties of endogenous AMPAR in CA1 pyramidal cells can be directly modified by increased αCaMKII activity.

To assess the contribution to αCaMKII-induced potentiation produced by the various mechanisms examined in this study, we use the relationship between mean response, M, mean quantal size, q, and mean quantal content, m, given by $M = q \times m$. Furthermore, the quantal size is given by $q = \gamma \times n$, where γ is the average unit conductance and n is the average number of channels activated at a synapse (the number of channels multiplied by their mean open probability). Assuming synapse homogeneity, the ratios of values in αCaMKII$_{1-290}$-expressing over control cells, indicated by Δ, are given by $\Delta M = \Delta q \times \Delta m$ and $\Delta q = \Delta\gamma \times \Delta n$. From our experiments, $\Delta M = 3.73$, $\Delta\gamma = 16.9/11.0 = 1.53$, and $\Delta q = 11.6/5.9 = 2.0$. Thus, $\Delta m = 3.73/2.0 = 1.87$ and $\Delta n = 2.0/1.53 = 1.3$. We can therefore roughly estimate that the increase in transmission produced by increased αCaMKII activity is attributable to an ~87% increase in quantal content (which can be accounted for by the decrease in the proportion of silent synapses), and an ~53% and an ~30% increase in the conductance and number of opened AMPA receptors per synapse, respectively.

DISCUSSION

We have shown that enhanced CaMKII activity in CA1 neurons leads to a specific potentiation of AMPAR-mediated synaptic transmission. This potentiation involves a reduction in the proportion of silent synapses devoid of functional AMPAR as well as an increase in the quantal size of AMPAR-mediated EPSCs. These results are consistent with the described properties of LTP at excitatory synapses onto these cells, suggesting that CaMKII acts as an early transduction signal during LTP induction, which initiates several divergent paths of enhancement of AMPAR-mediated transmission.

The uncovering of silent synapses has been suggested to play a significant role in the expression of LTP at several central excitatory synapses (Isaac et al., 1995; Liao et al., 1995; Li and Zhuo, 1998; Rumpel et al., 1998; Poncer and Malinow, 2001). This model is supported by immunogold electron microscopic studies that revealed morphological evidence for synapses containing NMDAR and lacking AMPAR (Nusser et al., 1998; Petralia et al., 1999; Takumi et al., 1999). We have shown previously that recombinant GluR1 overexpressed in CA1 pyramidal cells can be delivered to synapses after expression of constitutively active CaMKII (Hayashi et al., 2000). This process requires interaction between the Thr-887 residue of the intracellular carboxy-tail of GluR1 and a PDZ domain, presumably of proteins contained in the postsynaptic density (Bezprozvanny and Maximov, 2001; Sheng, 2001). Such a mechanism is likely involved in the αCaMKII-induced delivery of native AMPAR at previously silent synapses, as described in the present study. We report that, in most cases, the proportion of synaptic failures detected at +40 and −60 mV was identical in cells expressing αCaMKII$_{1-290}$, suggesting that virtually all synapses expressed functional AMPAR.

However, several reports have demonstrated an increase in quantal size associated with LTP expression at excitatory synapses onto CA1 cells (Malinow, 1991; Liao et al., 1992; Manabe et

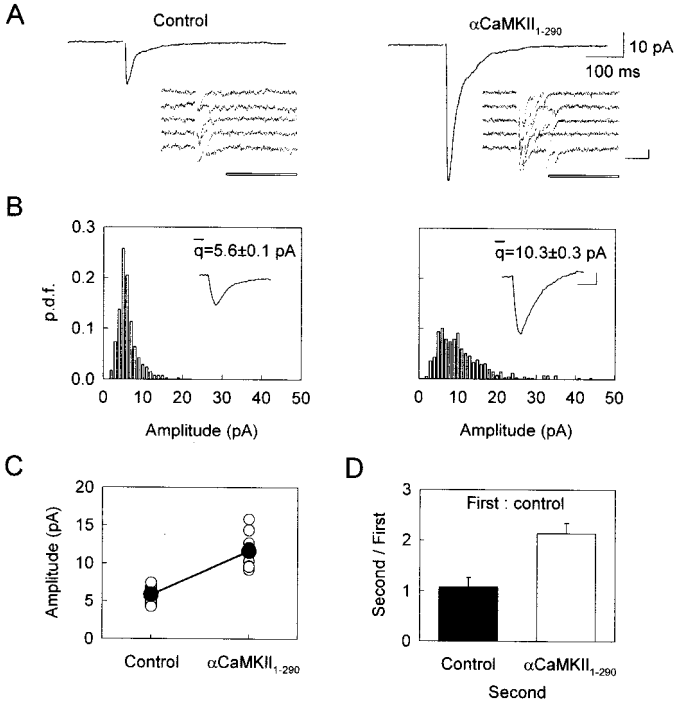

Figure 4. Increased quantal size of AMPAR EPSCs in pyramidal cells expressing αCaMKII$_{1-290}$–EGFP. EPSCs were evoked in pyramidal cells after substitution of Ca^{2+} by Sr^{2+}, resulting in asynchronous quantal events. *A*, EPSCs recorded in two neighboring CA1 cells (average of 200 consecutive EPSCs). *Inset*, Five consecutive responses showing asynchronous events after a larger initial event. *Open bars* show the section of *trace* that was used to detect quantal EPSCs. Calibration, 10 pA, 100 msec. *B*, Amplitude distributions of quantal EPSCs recorded in the two cells shown above. Note the shift of the distribution toward larger amplitudes in the cell expressing αCaMKII$_{1-290}$–EGFP. Consequently, the mean quantal size of EPSCs recorded in this cell, calculated as the average of quantal EPSC amplitudes, showed a ~83% increase compared with controls. Individual *traces* show the average of all detected quantal events (424 in controls, 418 in infected cells). Calibration, 2 pA, 10 msec. *p.d.f.*, Probability density function. *C*, Summary data for nine independent experiments (*open circles*). Note the increased variance of quantal size in infected cells. *Filled circles* indicate the average of all experiments. *D*, Graph showing the ratio of the quantal size of the first cell of a sequence over that of the second when the first cell was not infected and the second either uninfected as well (*filled bar*; $n = 5$) or infected (*open bar*; $n = 9$). Note the approximately twofold increase in quantal size when the second cell was infected, as in *C*.

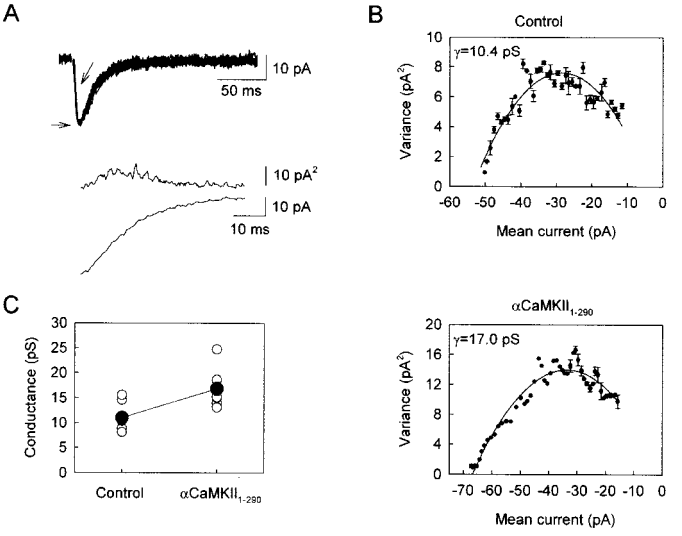

Figure 5. The unitary conductance of channels contributing to AMPAR EPSCs is increased in pyramidal cells expressing αCaMKII$_{1-290}$–EGFP. Nonstationary variance analysis was applied to locally evoked EPSCs onto control or infected pyramidal cells maintained at −60 mV, as described in Materials and Methods. *A*, A total of 30–45 EPSCs of similar amplitude were aligned to their half rising time and scaled in amplitude (*arrows*). The mean and variance of the currents were then computed for all data points of the decay phase, starting at the peak. *B*, Variance to mean relationship plotted for neighboring pyramidal neurons, both infected (*bottom*) and noninfected (*top*). Data points were binned according to mean current (see Materials and Methods). The unitary conductance of channels contributing to EPSCs in the infected cell was ~60% larger than the conductance derived from EPSCs in a neighboring control cell. *C*, Summary plots from nine independent experiments (*open circles*). *Filled circles* show the average conductance for control and infected cells (11.0 ± 0.8 and 16.9 ± 1.3 pS, respectively; $p < 0.002$).

al., 1992; Oliet et al., 1996; Stricker et al., 1996). A similar effect was observed with expression of αCaMKII$_{1-290}$ in our experiments (Fig. 4). An increase in quantal size could reflect an increased conductance of channels underlying AMPAR-mediated transmission, an increased number of receptors per synapse, or both. An increase in conductance can be detected with LTP of dendritically evoked EPSCs in CA1 pyramidal cells (Benke et al., 1998). Here, we show that the conductance of synaptic AMPAR channels is increased by ~50% in cells expressing αCaMKII$_{1-290}$. Phosphorylation of GluR1 by CaMKII is likely involved in this effect. The Ser-831 residue has been shown to be specifically phosphorylated by αCaMKII and during LTP (Barria et al., 1997a,b; Lee et al., 2000). Accordingly, we observed a >100% increase in Ser-831 phosphorylation in infected slices (data not shown). In a heterologous model, phosphorylation of Ser-831 or mutation to Asp on recombinant GluR1 results in increased channel conductance (Derkach et al., 1999). We therefore suggest that an increase in channel conductance underlies, at least in part, the increased quantal size associated with LTP and CaMKII activity in CA1 pyramidal neurons. An increase in either the number or the open probability of synaptic AMPARs is also likely to contribute to increasing quantal size. Indeed, the ~100% increase in quantal size associated with αCaMKII$_{1-290}$ expression (Fig. 4) may not be entirely accounted for by the ~50% increase in channel conductance we report (Fig. 5). Coexpression of a constitutively active CaMKII in human embryonic kidney cells expressing a recombinant GluR1, however, did not lead to any significant change in channel open probability (Derkach et al., 1999). We therefore suggest that the increased number of channels underlying mEPSCs in cells expressing αCaMKII$_{1-290}$ more likely reflects an increased number of receptors per synapse than an increased channel open probability. Immunogold electron microscopy using antibodies raised against AMPAR subunits may help resolve this issue.

In conclusion, our results provide additional support to the view that activation of CaMKII suffices to mimic the synaptic effects observed during LTP (Lledo et al., 1995). Of the increase in transmission produced by active CaMKII, approximately one-half is attributable to increased quantal content after conversion of silent synapses. The remaining potentiation is attributable to an increase in quantal size; approximately two-thirds of the increase in quantal size can be attributed to increased single-channel conductance, and the remainder can be attributed to an increase in receptor number. The increased conductance likely involves direct phosphorylation of GluR1. It remains to be determined whether CaMKII can phosphorylate and thereby increase

the conductance of synaptic receptors, or whether this modification occurs before receptor incorporation into synapses.

REFERENCES

Barria A, Muller D, Derkach V, Griffith LC, Soderling TR (1997a) Regulatory phosphorylation of AMPA-type glutamate receptors by CaM-KII during long-term potentiation. Science 276:2042–2045.

Barria A, Derkach V, Soderling T (1997b) Identification of the Ca^{2+}/calmodulin-dependent protein kinase II regulatory phosphorylation site in the α-amino-3-hydroxyl-5-methyl-4-isoxazole-propionate-type glutamate receptor. J Biol Chem 272:32727–32730.

Behrends JC, ten Bruggencate G (1998) Changes in quantal size distributions upon experimental variations in the probability of release at striatal inhibitory synapses. J Neurophysiol 79:2999–3011.

Benke TA, Luthi A, Isaac JT, Collingridge GL (1998) Modulation of AMPA receptor unitary conductance by synaptic activity. Nature 393:793–797.

Bezprozvanny I, Maximov A (2001) PDZ domains: more than just a glue. Proc Natl Acad Sci USA 98:787–789.

Braun AP, Schulman H (1995) The multifunctional calcium/calmodulin-dependent protein kinase: from form to function. Annu Rev Physiol 57:417–445.

Derkach V, Barria A, Soderling TR (1999) Ca^{2+}/calmodulin-kinase II enhances channel conductance of α-amino-3-hydroxy-5-methyl-4-isoxazolepropionate type glutamate receptors. Proc Natl Acad Sci USA 96:3269–3274.

Fukunaga K, Muller D, Miyamoto E (1995) Increased phosphorylation of Ca^{2+}/calmodulin-dependent protein kinase II and its endogenous substrates in the induction of long-term potentiation. J Biol Chem 270:6119–6124.

Goda Y, Stevens CF (1994) Two components of transmitter release at a central synapse. Proc Natl Acad Sci USA 91:12942–12946.

Hayashi Y, Shi SH, Esteban JA, Piccini A, Poncer JC, Malinow R (2000) Driving AMPA receptors into synapses by LTP and CaMKII: requirement for GluR1 and PDZ domain interaction. Science 287:2262–2267.

Hinds HL, Tonegawa S, Malinow R (1998) CA1 long-term potentiation is diminished but present in hippocampal slices from α-CaMKII mutant mice. Learn Mem 5:344–354.

Isaac JT, Nicoll RA, Malenka RC (1995) Evidence for silent synapses: implications for the expression of LTP. Neuron 15:427–434.

Kauer JA, Malenka RC, Nicoll RA (1988) A persistent postsynaptic modification mediates long-term potentiation in the hippocampus. Neuron 1:911–917.

Kullmann DM (1994) Amplitude fluctuations of dual-component EPSCs in hippocampal pyramidal cells: implications for long-term potentiation. Neuron 12:1111–1120.

Kullmann DM, Nicoll RA (1992) Long-term potentiation is associated with increases in quantal content and quantal amplitude. Nature 357:240–244.

Lee HK, Barbarosie M, Kameyama K, Bear MF, Huganir RL (2000) Regulation of distinct AMPA receptor phosphorylation sites during bidirectional synaptic plasticity. Nature 405:955–959.

Li P, Zhuo M (1998) Silent glutamatergic synapses and nociception in mammalian spinal cord. Nature 393:695–698.

Liao D, Jones A, Malinow R (1992) Direct measurement of quantal changes underlying long-term potentiation in CA1 hippocampus. Neuron 9:1089–1097.

Liao D, Hessler NA, Malinow R (1995) Activation of postsynaptically silent synapses during pairing-induced LTP in CA1 region of hippocampal slice. Nature 375:400–404.

Linden DJ (2001) The expression of cerebellar LTD in culture is not associated with changes in AMPA-receptor kinetics, agonist affinity, or unitary conductance. Proc Natl Acad Sci USA 98:14066–14071.

Lisman J, Malenka RC, Nicoll RA, Malinow R (1997) Learning mechanisms: the case for CaM-KII. Science 276:2001–2002.

Lledo PM, Hjelmstad GO, Mukherji S, Soderling TR, Malenka RC, Nicoll RA (1995) Calcium/calmodulin-dependent kinase II and long-term potentiation enhance synaptic transmission by the same mechanism. Proc Natl Acad Sci USA 92:11175–11179.

Malgaroli A, Tsien RW (1992) Glutamate-induced long-term potentiation of the frequency of miniature synaptic currents in cultured hippocampal neurons. Nature 357:134–139.

Malinow R (1991) Transmission between pairs of hippocampal slice neurons: quantal levels, oscillations, and LTP. Science 252:722–724.

Malinow R, Tsien RW (1990) Presynaptic enhancement shown by whole-cell recordings of long-term potentiation in hippocampal slices. Nature 346:177–180.

Malinow R, Hayashi Y, Maletic-Savatic M, Zaman SH, Poncer JC, Shi SH, Esteban JA (1999) Introduction of green fluorescent protein into hippocampal neurons through viral infection. In: Imaging neurons: a laboratory manual (Yuste R, Lanni F, Konnerth A, eds), pp 58.1–58.8. Cold Spring Harbor, NY: Cold Spring Harbor Laboratory.

Mammen AL, Kameyama K, Roche KW, Huganir RL (1997) Phosphorylation of the α-amino-3-hydroxy-5-methylisoxazole4-propionic acid receptor GluR1 subunit by calcium/calmodulin-dependent kinase II. J Biol Chem 272:32528–32533.

Manabe T, Renner P, Nicoll RA (1992) Postsynaptic contribution to long-term potentiation revealed by the analysis of miniature synaptic currents. Nature 355:50–55.

Meyer T, Hanson PI, Stryer L, Schulman H (1992) Calmodulin trapping by calcium-calmodulin-dependent protein kinase. Science 256:1199–1202.

Miller SG, Patton BL, Kennedy MB (1988) Sequences of autophosphorylation sites in neuronal type II CaM kinase that control Ca^{2+}-independent activity. Neuron 1:593–604.

Muller D, Lynch G (1988) Long-term potentiation differentially affects two components of synaptic responses in hippocampus. Proc Natl Acad Sci USA 85:9346–9350.

Nusser Z, Lujan R, Laube G, Roberts JD, Molnar E, Somogyi P (1998) Cell type and pathway dependence of synaptic AMPA receptor number and variability in the hippocampus. Neuron 21:545–559.

Oliet SH, Malenka RC, Nicoll RA (1996) Bidirectional control of quantal size by synaptic activity in the hippocampus. Science 271:1294–1297.

Ouyang Y, Rosenstein A, Kreiman G, Schuman EM, Kennedy MB (1999) Tetanic stimulation leads to increased accumulation of Ca^{2+}/calmodulin-dependent protein kinase II via dendritic protein synthesis in hippocampal neurons. J Neurosci 19:7823–7833.

Petralia RS, Esteban JA, Wang YX, Partridge JG, Zhao HM, Wenthold RJ, Malinow R (1999) Selective acquisition of AMPA receptors over postnatal development suggests a molecular basis for silent synapses. Nat Neurosci 2:31–36.

Pettit DL, Perlman S, Malinow R (1994) Potentiated transmission and prevention of further LTP by increased CaMKII activity in postsynaptic hippocampal slice neurons. Science 266:1881–1885.

Poncer JC, Malinow R (2001) Postsynaptic conversion of silent synapses during LTP affects synaptic gain and transmission dynamics. Nat Neurosci 4:989–996.

Rumpel S, Hatt H, Gottmann K (1998) Silent synapses in the developing rat visual cortex: evidence for postsynaptic expression of synaptic plasticity. J Neurosci 18:8863–8874.

Sheng M (2001) Molecular organization of the postsynaptic specialization. Proc Natl Acad Sci USA 98:7058–7061.

Shirke AM, Malinow R (1997) Mechanisms of potentiation by calcium-calmodulin kinase II of postsynaptic sensitivity in rat hippocampal CA1 neurons. J Neurophysiol 78:2682–2692.

Silva AJ, Stevens CF, Tonegawa S, Wang Y (1992) Deficient hippocampal long-term potentiation in α-calcium-calmodulin kinase II mutant mice. Science 257:201–206.

Soderling TR, Derkach VA (2000) Postsynaptic protein phosphorylation and LTP. Trends Neurosci 23:75–80.

Stricker C, Field AC, Redman SJ (1996) Changes in quantal parameters of EPSCs in rat CA1 neurones in vitro after the induction of long-term potentiation. J Physiol (Lond) 490:443–454.

Takumi Y, Ramirez-Leon V, Laake P, Rinvik E, Ottersen OP (1999) Different modes of expression of AMPA and NMDA receptors in hippocampal synapses. Nat Neurosci 2:618–624.

Traynelis SF, Silver RA, Cull-Candy SG (1993) Estimated conductance of glutamate receptor channels activated during EPSCs at the cerebellar mossy fiber-granule cell synapse. Neuron 11:279–289.